Channel flow over a compliant wall

M. Manning, B. Bamieh

August 10, 2007

1 Introduction

In 1960 Kramer [8, 9] published a series of papers describing experiments where he covered an underwater object with rubber and found considerable reductions in the drag. Experiments have been conducted to study other flows past compliant boundaries — blood flow in arteries, dolphin propulsion, etc. Since then, there has been significant theoretical effort expended to understand how compliant walls affect hydrodynamic stability. The first papers by Benjamin [2] and Landahl [11] and more recent papers [4, 6, 10] study two-dimensional (streamwise and wall-normal) flow using standard stability analysis.

The starting point for these studies is Tollmien-Schlicting (TS) waves, which are the most unstable modes of the 2D linearized Navier Stokes (LNS) operator for channel and Blasius boundary layer flow. In a certain parameter range, the flexible wall modifies and stabilizes these "Class A" streamwise undulating waves. The flexible wall also supports surface waves with a characteristic wavespeed; in another parameter range the fluid excites these "Class B" modes in the wall and the system becomes unstable [2, 11]. Essentially, then, stability is enhanced in a small parameter range where Class A waves are suppressed and Class B waves are not excited. Carpenter and Garrad highlight the fact that there is an additional "Class C" mode that occurs as a coalescence of Class A and Class B modes. This mode is call "standing wave flutter" and is an oscillating staing wave. [**?**].

An important question is whether these two-dimensional flow models capture the important details of three dimensional flow. For flow past a rigid wall, this is not the case. TS waves have been experimentally verified [**?**] in experiments with extremely low environmental noise and geometric irregularity. However, in many experiments researchers do not see TS waves but instead streamwise streaks and vortices [], which are *not* the unstable eigenfunctions of the respective linearized equations.

One explanation for this is that there may be eigenmodes of the LNS operator which experience large transient growth, even though they are linearly stable. This is possible because the LNS operator is highly non-normal at high Reynolds number, and therefore its eigenmodes are non-orthogonal. In this case small perturbations to laminar flow can be significantly amplified so that the orginal linearized description is no longer valid.

These ideas were perhaps first highlighted by Butler and Farell [3], who studied perturbations to the initial conditions of the system, and later by Trefethen et. al [13] who studied perturbations to the differential operator itself. Other studies have confirmed that non-normal, stable modes of the LNS operator undergo large transient growth []. Borrowing tools from control theory, "Input/output"(I/O) analysis provides an algorithmic method for incorporating uncertainty as input body forces and pinpointing energy amplification in the system [**?**, **?**]. It can be shown that "input-output" analysis encompasses both "optimal perturbation" methods and "psedospectral" analyses. The goal of the analysis is to find the "most resonant modes" — those modes which are most likely to result from amplification of small perturbations.

A study by Jovanovic and Bamieh of the 3D LNS equations [**?**] shows that streamwise vortices are the "most resonant mode" in rigid-wall channel flows. This agrees with flow structures seen in transition to turbulence in noisy experiments, and suggests a novel approach for studying transition to turbulence in flow past compliant walls. In this paper, we perform an input-output analysis of a simplified channel flow model (2D/3C) that captures the energy amplification seen in full three-dimensional models. We show that ....

The paper is organized as follows. In Section 2, we review the spectral theorem for normal, linearized operators, and discuss how transient growth is possible for linearly stable eigenmodes of non-normal operators. We also discuss how Input-Output analysis identifies this transient amplification. In Section 3 we discuss our simplified model for the fluid and the compliant wall, and linearize the system about planar Couette flow, and implement the system in MATLAB using descriptor notation. In Section **??** we use I/O analysis as a tool to understand the natural modes of the wall, and arrive at a more detailed understanding of the surface waves described by Benjamin [2]. Section **??** describes an I/O analysis of the fluid coupled to a compliant boundary. We first investigate a simple Kramer-type boundary [**?**, **?**], and later expand the model to allow stretching in the spanwise direction, as first explored in [12].

2 Background: Linear and Input-Output stability analysis

Linear stability is often used to understand and predict the behavior of dynamical systems. The goal is to find eigenvalues of a linearized dynamical operator. Eigenvalues with negative real parts correspond to eigenmodes that will eventually decay, and a system where all the eigenmodes eventually decay is linearly stable. This technique usually makes correct predictions, but there are several important instances where it is known to fail – channel and pipe flows, for example. One way to explain this failure is to say that the linear operator is highly sensitive to small perturbations or model uncertainty. We can still study the linear operator to predict system behavior, by adding a disturbance input to the operator and seeing what types of perturbations are most ampli-

fied. This disturbance input can mimic inhomogeneous boundaries and model uncertainty as well as perturbations to initial conditions. Although all perturbations must eventually decay, certain *resonant* perturbations can be transiently amplified by large factors if the linear operator is non-normal (eigenmodes are non-orthogonal). This amplification of the "most resonant modes" is easily studied using input-output (I/O) techniques from control theory in engineering.

Given a dynamical system described by the following linear equation:

$$\dot{x} = Ax, \tag{1}$$

it is well-known that if A is a normal linear operator and all of its eigenvalues have negative real parts, then eigenmodes of A decay monotonically and the system is aymptotically stable. However, this is not true for *non-normal* linear operators. The fact that the eigenmodes of these operators are not orthogonal has important implications for stability and transient growth.

Recall that an operator A is normal if it satisfies the equation $AA^T = A^TA$. A consequence of this definition is that A has orthogonal eigenvectors that span R^n and therefore A is diagonalizable. We can find an change of variables $x = Sy$ such that $\dot{y} = S^{-1}ASy$ and $S^{-1}AS$ is diagonal. This implies that the dynamics of each component are decoupled,

$$\dot{y_j} = \lambda_j y_j \quad j \in 1 \dots n, \tag{2}$$

and each component has the solution

$$y_j = y_{j0} e^{\lambda_j t}. \tag{3}$$

Obviously, if all the λ_j have negative real parts, then each eigenmode decays exponentially. Note that Hermitian and unitary operators are both normal, which may explain why scientists and engineers are so familiar with this behavior.

Non-normal operators may or may not be diagonalizable, and we can not always describe them as a series of decoupled eigenmodes. We can build some intuition about these operators by examining a specific example. Let A be defined as:

$$A = \begin{bmatrix} \lambda_1 & \mathcal{N} \\ 0 & \lambda_2 \end{bmatrix}. \tag{4}$$

Because the matrix is upper triangular, λ_1 and λ_2 are its eigenvalues, and the eigenmodes are the following vectors:

$$e_1 = \begin{bmatrix} 1 \\ 0 \end{bmatrix}; \quad e_2 = \begin{bmatrix} \mathcal{N}/(\lambda_1 - \lambda_2) \\ 1 \end{bmatrix}; \tag{5}$$

Note that e_1 and e_2 are linearly independent (unless $\lambda_1 = \lambda_2$), but as $\mathcal{N}$ increases they become more and more parallel to one another. In this sense, $\mathcal{N}$ can be considered a measure of the non-normality of the operator A. Even if A is linearly stable (λ_1 and λ_2 both negative), a perturbation $\boldsymbol{u} = (u_1, u_2)$ can grow

transiently if $\mathcal{N}$ is large enough:

$$\begin{aligned} \partial_t u_1 &= \left[u_1 + u_2 \frac{\mathcal{N}}{(\lambda_1 - \lambda_2)} \left(e^{(\lambda_1 - \lambda 2)t} - 1 \right) \right] e^{\lambda_1 t} \\ \partial_t u_2 &= u_2 e^{\lambda_2 t} \end{aligned} \tag{6}$$

Figure 1 shows the vector field of the nonnormal operator A and time evolution of an initial perturbation $\boldsymbol{u} = (0.5, 0.5)$ acted upon by that operator. Non-

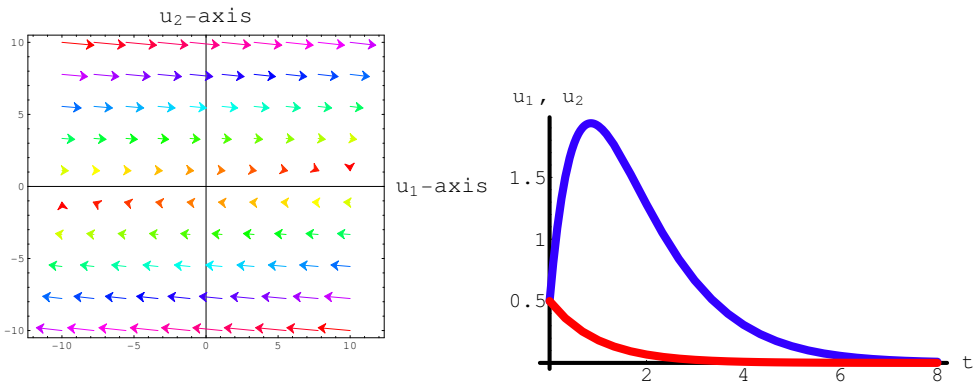

Figure 1: a) Vector Field of operator A given by Eq. 4, with $\lambda_1 = -1.1$, $\lambda_2 = -1$, $\mathcal{N} = 10$. b) Time evolution of an initial perturbation $\boldsymbol{u} = (0.5, 0.5)$ acted upon by A.

normal operators can exhibit large transient behavior in the presence of small perturbations, even when those operators are linearly stable. This mechanism can be used to explain why linear stability analysis fails in some shear flows.

3 Model equations for the fluid/wall system

3.1 2D/3C

In the full 3D system with rigid walls, Jovanovic and Bamieh found that the spanwise periodicity is much smaller than the streamwise periodicity, suggesting that the most resonant modes can be approximated by streamwise *constant* structures. This possibility was first explored by Bobba et al. [7]. These authors consider a system which has streamwise constant flow perturbations in three dimensional plane couette flow. This results in a two-dimensional model (in y and z) which contains all three components of the velocity (u, v, w), called the two-dimensional/three component (2D/3C) model. This 2D model is different from most 2D hydrodynamic models which study the wall-normal (y) and streamwise (x) directions; we study a *cross-section* of the channel in the wall-normal and spanwise directions. Numerical simulations indicate that the 2D/3C model does

an excellent job of capturing the resonant modes found in the full 3-D analysis, while greatly simplifying the expressions.

In this work we modify the 2D/3C model so the bottom wall of the channel is no longer fixed, but is instead a compliant/flexible wall that can interact with the flow moving over it. A schematic diagram is shown in Figure 2.

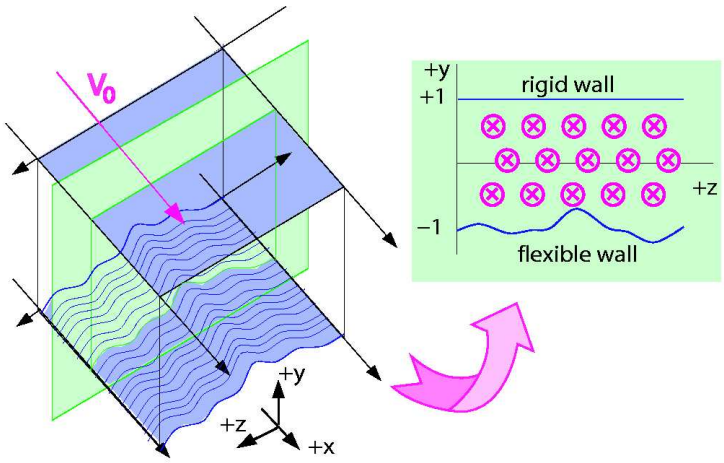

Figure 2: Illustration of geometry for 2D/3C model with flexible boundary

Motivated by 3D simulations for the rigid wall case, we assume that the important interactions between the wall and fluid are approximately streamwise constant. It is possible that the flexible wall causes perturbations with small streamwise periodicity to become important(which is the focus of work by Bejamin, Landahl and others [2, 11]), but we do not consider that possibility here. The 2D/3C model is an analytically tractable starting point for this analysis, but a more complicated 3D model could capture additional features and should be an avenue for future study.

Our goal is find the LNS operator which describes the 2D/3C model for channel flow with a flexible boundary. We then analyze this operator using input/output techniques to determine the effect of the flexible wall (and wall parameters) on the amplification of the *most resonant modes.*

In this section we develop equations for the 2D/3C dynamics of the fluid as well as the compliant, flexible wall. In the following section we nondimensionalize the equations, and linearize the system around steady state channel flow. Section IV describes the steps necssary to numerically represent the linearized operator, including homogenizing the boundary conditions and representing the pressure in terms of other state variables. Finally, we evaluate the generalized

stability of the linearized operator.

3.2 Linearized 2D/3C Equations for the fluid

We use the three-dimensional nonlinear incompressible Navier-Stokes (NS) equations to describe the dynamics of the fluid dynamics in the bulk. The interaction between the wall and the fluid enters these equations through the boundary conditions, and therefore doesn't affect the conservation or constitutive equations for the bulk fluid. The NS equations are:

$$\begin{aligned} \rho^*(\partial_t^*\mathbf{v}^* + \nabla_{\mathbf{v}^*}^*\mathbf{v}^*) &= -\nabla^* p^* + \eta^*\nabla^{*2}\mathbf{v}^* + \mathbf{d}^* \quad (7) \\ 0 &= \nabla^* \cdot \mathbf{v}^* \quad (8) \end{aligned}$$

where $\mathbf{v}^*$ is the fluid velocity field, ρ^* is the fluid volummetric density, and η^* is the viscosity. Throughout this paper we use the convention that starred variables are dimensional and unstarred variables are dimensionless. These equations contain an additional body force, denoted $\mathbf{d}^*$. This *input uncertainty* term enables us to analyze how small body forces might dramatically change the system behavior. These body forces could be caused by external vibrations, air currents, wall roughness, small obstacles, and can even be used to capture model uncertainty. We will return to these input forces in Section V.

For a channel flow, we can analyze the linearized dynamics of the fluid velocities about a flow state composed of a purely streamwise component, denoted V_0. Using the 2D/3C model and linearizing Eq. (7) about V_0 results in simple equations for the three components of the fluid velocity, v_x, v_y, v_z:

$$\begin{aligned} \rho^*\frac{\partial v_x^*}{\partial t^*} &= -\rho^* V_0^{*\prime} v_y^* + \eta^*\nabla^{2*} v_x^*; \quad (9) \\ \rho^*\frac{\partial v_y^*}{\partial t^*} &= -\frac{\partial p^*}{\partial y^*} + \eta^*\nabla^{2*} v_y^*; \quad (10) \\ \rho^*\frac{\partial v_z^*}{\partial t^*} &= -\frac{\partial p^*}{\partial z^*} + \eta^*\nabla^{2*} v_z^*. \quad (11) \end{aligned}$$

Conservartion of momentum, Eq. 16, yields an additional constraint:

$$0 = \frac{\partial v_y^*}{\partial y^*} + \frac{\partial v_z^*}{\partial z^*}. \quad (12)$$

As customary for channel flows, we nondimensionalize the equations so that the remaining parameter is the Reynolds number, $Re = (V_0^* L^* \rho^*)/\eta^*$. In this case,

the equations are:

$$\frac{\partial v_x}{\partial t} = -V_0' v_y + \frac{1}{Re}\nabla^2 v_x; \tag{13}$$

$$\frac{\partial v_y}{\partial t} = -\frac{\partial p}{\partial y} + \frac{1}{Re}\nabla^2 v_y; \tag{14}$$

$$\frac{\partial v_z}{\partial t} = -\frac{\partial p}{\partial z} + \frac{1}{Re}\nabla^2 v_z; \tag{15}$$

$$0 = \frac{\partial v_y}{\partial y} + \frac{\partial v_z}{\partial z}, \tag{16}$$

where p is defined by $p^* = p\rho V_0^2$.

The partial differential equations for the fluid velocities require boundary conditions. Let the upper boundary be a flat wall at $y = y^+ = 1$, while the lower boundary is displaced a distance $u_y(x, z, t)$.

$$y = y^- = -1 + u_y(x, z, t). \tag{17}$$

We enforce a no-slip boundary condition:

$$v_i(x, y = y^+, z, t) = \frac{\partial u_i}{\partial t} = 0, \quad i = x, y, z. \tag{18}$$

3.3 Compliant wall model

There are many possible models for the compliant wall: an elastic half-space, viscoelastic fluid, and tensioned sheet are just a few of the examples found in the literature [2, 11]. We will use a plate-membrane model for the wall, which consists of a spring-backed sheet under tension that dissipates energy proportional to the velocity. While this model might have been first used to model dolphin skin [**?**], it can be used to describe many other systems. The plate spring model encompasses many simpler models, and in this paper we invesitgate simpler models by setting various model parameters to zero.

In the majority of previous studies, the wall is constrained to move only in the wall-normal direction, while the tangential motion is ignored. However, Thaokar, Shankar and Kumaran have shown that the spanwise tangential component of motion in the membrane is critical in understanding low Reynolds number 2D fluid flow. [12] In this investigation we permit the wall to stretch in both streamwise and spanwise directions.

A starting point for the plate-membrane model is an elastic sheet – a 2D lattice of masses in x and z that are confined by a harmonic potential in the limit that the lattice spacing goes to zero. The model assumes that energy is dissipated in the solid at a rate proportional to the velocity individual lattice points. In the 2D/3C model, all displacement fields must be constant in the x-drection. This results in three equations for the three component of the wall displacement, u_x, u_y, and u_z:

$$\sigma^* \ddot{u}_i^*(z) + D_i^* \dot{u}_i^*(z) = f_i^* + T_i^* \frac{\partial^2 u_i^*(z)}{\partial z^*} \quad i = 1, 2, 3, \tag{19}$$

where σ^* is the areal mass density of the wall, D_i^* is a damping coefficient density, T_i^* is a tension and f_i is the sum of external stresses in the i-direction. A derivation of these equations can be found in Appendix **??**

This is essentially the model used by Benjamin and Landahl. The simple elastic model misses some features of real materials. This model contains no energy penalty for bending in the wall-normal direction or for uniform translation. The first problem is corrected by adding a bending term, with energy density E_y to the potential energy. The second problem is solved by adding spring tethers with spring constant J_i that attach each node to a point in physical space. (These are different from the springs that connect nodes.) In [12], the wall-plate model contains tethers in the wall-normal direction but not the streamwise direction, which leads to a linearly unstable mode where the wall translates in the streamwise direction.

We nondimensionalize the resulting 2D/3C wall model, which is described by the following system of equations:

$$\begin{aligned}
\sigma\ddot{u}_x(z) + D_x\dot{u}_x(z) &= f_x + T_x\frac{\partial^2 u_x}{\partial z} - \mathcal{J}_x u_x, && (20)\\
\sigma\ddot{u}_y(z) + D_y\dot{u}_y(z) &= f_y + T_y\frac{\partial^2 u_y}{\partial z} - \mathcal{J}_y u_y - E_y\frac{\partial^4 u_y}{\partial z^4}, && (21)\\
\sigma\ddot{u}_z(z) + D_x\dot{u}_z(z) &= f_z + T_z\frac{\partial^2 u_z}{\partial z} - \mathcal{J}_z u_z. && (22)
\end{aligned}$$

where $\mathcal{J}_i$ is the tethering spring constant and E_y is a bending energy density. These terms are also derived in Appendix **??**. A schematic diagram of the model geometry is shown in figure **??**.

The wall is being forced by the fluid, and possibly by disturbance body forces (noise) not explicitly included in our model, which we denote as $\boldsymbol{d_{wi}}$. The fluid forcing is determined by the components of fluid stress tensor $\boldsymbol{\tau}_{\mathrm{fl}}^*$ evaluated at the fluid-wall interface. Due to the wall-normal displacement u_y, the interface is no longer oriented parallel to the x-z plane. Taking this effect into account, the body forces are:

$$\begin{aligned}
f_x^* &= (\widehat{n_x}\cdot\boldsymbol{\tau}_{\mathrm{fl}}^*\cdot\widehat{n_y})|_{y=-1} + d_{wx}^*,\\
f_y^* &= (\widehat{n_y}\cdot\boldsymbol{\tau}_{\mathrm{fl}}^*\cdot\widehat{n_y})|_{y=-1} + d_{wy}^*,\\
f_z^* &= (\widehat{n_z}\cdot\boldsymbol{\tau}_{\mathrm{fl}}^*\cdot\widehat{n_y})|_{y=-1} + d_{wz}^* \qquad (23)
\end{aligned}$$

where the vectors n_i that desribe the tangent plane are given to first order in the perturbations by:

$$\begin{aligned}
\widehat{n_x} &= \hat{\mathrm{x}} + \partial_x^* u_y^*\,\hat{\mathrm{y}} + 0\,\hat{\mathrm{z}};\\
\widehat{n_y} &= -\partial_x^* u_y^*\,\hat{\mathrm{x}} + \hat{\mathrm{y}} - \partial_z^* u_y^*\,\hat{\mathrm{z}};\\
\widehat{n_z} &= 0\,\hat{\mathrm{x}} + \partial_z^* u_y^*\,\hat{\mathrm{y}} + \hat{\mathrm{z}}. \qquad (24)
\end{aligned}$$

3.4 Linearization of fluid/wall system about planar Couette flow

A particularly simple steady state for channel flow with rigid walls is Couette flow – boundary driven flow with a velocity field that is purely streamwise with a linear wall-normal profile. Convieniently, planar couette flow is also a steady state solution for a fluid flow past the plate-spring model. Let the boundaries at $\pm L$ be driven at a velocity $\pm V_0$. The steady state solution to this flow, denoted $\overline{\phi}$, is $v_x(y) = y$, with all other velocities and displacements equal to zero. The nominal pressure is also zero, because this is the only value for the pressure consistent with $\partial_x p = \partial_y p = partial_z p = 0$ and $u_y = 0$.

Let $\phi = \overline{\phi} + \widetilde{\phi}$, where $\widetilde{\phi}$ is a vector of perturbed state variables. We will assume the perturbations are small, and linearize the system of equations by ignoring terms which are second order in the perturbations. Conservation of fluid mass and momentum, Eqs. (13), (14), (15), and (16) govern the fluid velocities, while Eqs. (20), (21) and (22) govern the wall postions and velocities. The two systems are coupled through the boundary conditions, Eq. (18), and the fluid stresses, $\tau^*_{ij\,fl}$, which we must express in terms of the other variables. The total stress tensor for a Newtonian fluid in Couette flow is simply related to the fluid velocity and pressure fields:

$$\tau^*_{ij\,fl} = \eta^* \left(\partial^*_i v^*_j + \partial^*_j v^*_i\right) - p^* \delta_{ij} \tag{25}$$

We can expand this expression, keeping only first order terms in the perturbation fields:

$$\boldsymbol{\tau_{fl}} = \begin{bmatrix} -p^* & \eta\left(\partial^*_y v^*_x + V^*_0/L\right) & \eta\partial^*_z v^*_x \\ \eta\left(\partial^*_y v^*_x + V^*_0/L\right) & -p^* + 2\eta\partial^*_y v^*_y & \eta(\partial^*_z v^*_y + \partial^*_y v^*_z) \\ \eta\partial^*_z v^*_x & \eta(\partial^*_z v^*_y + \partial^*_y v^*_z) & -p^* + 2\eta\partial^*_y v^*_y \end{bmatrix}.$$

Note that the pressure p^* is the perturbed pressure field, as the nominal pressure field is zero. The spatial average of this field does not have to be zero. However, the value of the pressure (as opposed to its derivatives) only enters the equations of motions through Eq. 3.4. *Note: for awhile we assumed that the perturbation pressure had to have a zero average in the y-direction... this simply isn't true, and doesn't give the correct answer for the MSV in the limit of a very rigid wall.*

Substituting in to Eq. 23 we find:

$$f^*_x = \frac{\eta V^*_0}{L} + \eta\partial_y v_x + d_{wx}; \tag{26}$$

$$f^*_y = -p + 2\eta\partial_y v_y + d_{wy}; \tag{27}$$

$$f^*_z = \eta\left(\partial_z v_y + \partial_y v_z\right) + d_{wz}. \tag{28}$$

Nondimensionalizing these equations and substituting into Eqs. (20), (21), (22),

and (3.4) results in the following equations for the linearized wall dynamics.

$$\sigma\partial_t s_x = -D_x s_x + V_0 + \partial_y v_x + d_{wx} + T_x\frac{\partial^2 u_x}{\partial z} - \mathcal{J}_x u_x, \tag{29}$$

$$\sigma\partial_t s_y = -D_y s_y + -p + 2\partial_y v_y + d_{wy} + T_y\frac{\partial^2 u_y}{\partial z} - \mathcal{J}_y u_y - E_y\frac{\partial^4 u_y}{\partial z^4}, \tag{30}$$

$$\sigma\partial_t s_z(z) = -D_x \dot{u_z}(z) + (\partial_z v_y + \partial_y v_z) + d_{wz} + T_z\frac{\partial^2 u_z}{\partial z} - \mathcal{J}_z u_z. \tag{31}$$

The dynamics of the linearized system can be written in matrix form:

$$\partial_t \begin{bmatrix} v_x \\ v_y \\ v_z \\ u_x \\ u_y \\ u_z \\ s_x \\ s_y \\ s_z \end{bmatrix} = \begin{bmatrix} \Delta/Re & -V_0 & 0 & 0 & 0 & 0 & 0 & 0 & 0 \\ 0 & \Delta/Re & 0 & 0 & 0 & 0 & 0 & 0 & 0 \\ 0 & 0 & \Delta/Re & 0 & 0 & 0 & 0 & 0 & 0 \\ 0 & 0 & 0 & 0 & 0 & 0 & 1 & 0 & 0 \\ 0 & 0 & 0 & 0 & 0 & 0 & 0 & 1 & 0 \\ 0 & 0 & 0 & 0 & 0 & 0 & 0 & 0 & 1 \\ \partial_y/\sigma|_{y=-1} & 0 & 0 & \gamma_x & 0 & 0 & -D_x/\sigma & 0 & 0 \\ 0 & 2\partial_y/\sigma|_{y=-1} & 0 & 0 & \gamma_y & 0 & 0 & -D_y/\sigma & 0 \\ 0 & \partial_z/\sigma|_{y=-1} & \partial_y/\sigma|_{y=-1} & 0 & 0 & \gamma_z & 0 & 0 & -D_z/\sigma \end{bmatrix} \begin{bmatrix} v_x \\ v_y \\ v_z \\ u_x \\ u_y \\ u_z \\ s_x \\ s_y \\ s_z \end{bmatrix}$$

$$- \begin{bmatrix} 0 \\ \partial_y \\ \partial_z \\ 0 \\ 0 \\ 0 \\ 0 \\ 1/\sigma|_{y=-1} \\ 0 \end{bmatrix} \tilde{p} - \begin{bmatrix} 0 \\ 0 \\ 0 \\ 0 \\ 0 \\ 0 \\ 0 \\ 1/\sigma|_{y=-1} \\ 0 \end{bmatrix} \overline{p} + \frac{1}{\rho} \begin{bmatrix} d_{fx} \\ d_{fy} \\ d_{fz} \\ 0 \\ 0 \\ 0 \\ 0 \\ 0 \\ 0 \end{bmatrix} \tag{32}$$

$$0 = \begin{bmatrix} 0 & \partial_y & \partial_z & 0 & 0 & 0 & 0 & 0 & 0 \end{bmatrix} \begin{bmatrix} v_x \\ v_y \\ v_z \\ u_x \\ u_y \\ u_z \\ s_x \\ s_y \\ s_z \end{bmatrix} \tag{33}$$

$$+ \quad \text{Boundary Conditions.}$$

where γ_i is defined as:

$$\gamma_i = \frac{-J_i + T_i\partial_z^2 - B_i\partial_z^4}{\sigma} \tag{34}$$

For notational simplicity, we define new matricies $\widetilde{A}$,$\widetilde{B}$,$\widetilde{D}$, and $\widetilde{Q}$, by com-

paring Eq. (32) to the following equation:

$$\begin{aligned} \dot{\phi} &= \widetilde{A}\phi + \widetilde{Q}p + \widetilde{B}d && (35)\\ 0 &= \widetilde{D}\phi && (36)\\ &+ \text{Boundary conditions} && (37) \end{aligned}$$

where the matricies A, Q, and D are defined by Eq. (32).

3.5 Conversion to a homogenous boundary problem

Unlike a rigid-wall flow, the velocity fields in Eq. (35) do not have Dirichlet boundary conditions because the fluid velocity is slaved to the wall velocity, as in Eq. (**??**). However, we re-write our system of equations in terms of state variables that DO have Dirichlet boundary conditions using a technique called "Homogenization of Boundary Conditions" [5, **?**]. We define new variables v_i^h, which do have Dirichlet BCs, in the following way:

$$v_i(y) \equiv v_i^h(y) + f(y)s_i, \tag{38}$$

where s_i is the wall velocity and $f(y) = 1/2\,(1-y)$ is the first degree polynomial that satisfies the boundary conditions: $f(+1) = 0, f(-1) = 1$. We can write this system of equations as a matrix equation: $\phi = M\phi^h$ and then re-write the originial system of equations (Eq. 35) as:

$$\begin{aligned} \dot{\phi^h} &= M^{-1}\widetilde{A}M\phi^h + M^{-1}\widetilde{Q}p + M^{-1}\widetilde{B}d; && (39)\\ \widetilde{D}M\phi^h &= 0. && (40) \end{aligned}$$

We can then incorporate the divergence constraint by writing the system in descriptor form. Descriptor notation is a way of expressing and solving differential-algebraic systems of equations developed in the context of controls. In an earlier paper [**?**], we showed that descriptor notation is well-suited to incompressible fluid flows and eliminates the spurious eigenvalues that often arise in these systems.

$$\begin{aligned} \begin{bmatrix} I & 0 \\ 0 & 0 \end{bmatrix} \begin{bmatrix} \dot{\phi^h} \\ \dot{p} \end{bmatrix} &= \begin{bmatrix} M^{-1}AM & M^{-1}Q \\ DM & 0 \end{bmatrix} \begin{bmatrix} \phi^h \\ p \end{bmatrix} + M^{-1}\widetilde{B}d; && (41)\\ \phi &= M\phi^h. && (42) \end{aligned}$$

3.6 Formulation as an input/output problem

We are now in a position to check the stability of the fluid-wall system as a function of wall parameters. The full fluid/wall system, Eq. 41 can now be written in input/output form:

$$\begin{aligned} E \begin{bmatrix} \dot{\phi^h} \\ \dot{p} \end{bmatrix} &= A \begin{bmatrix} \phi^h \\ p \end{bmatrix} + Bd; && (43)\\ \text{output} &= C \begin{bmatrix} \phi^h \\ p \end{bmatrix}, && (44) \end{aligned}$$

where the operators E, A, are defined by Eq. 41. We first check the linear stability of the (A, E) pair. if A, E is linearly stable, we then study the transient amplification of perturbations using input-output analysis.

We choose the input matrix B and the output matrix C in order to study the response of a specific component of the system. For example, we could study the response of the wall velocities to wall perturbations (i.e. flutter) by choosing B and C appropriately. In this paper, we focus on transition to turbulence in the fluid, and therefore investigate the response of the fluid velocities to fluid perturbations.

We restrict ourselves to body forces that act only on the fluid, and therefore the matrix B takes the following form:

$$\begin{aligned} B_{ij} &= 1, \quad i = j \in \{1, 2, 3\}; && (45) \\ &= 0, \quad \text{otherwise.} && (46) \end{aligned}$$

The kinetic energy density of a harmonic perturbation in the fluid, which is the same energy norm used in [**?**], is the $L^2[-1, 1]$ inner prodcut of the Fourier-transformed fluid velocity vector times the fluid mass density: $\rho\widehat{\boldsymbol{v}} = \rho[\widehat{v_x} \quad \widehat{v_y} \quad \widehat{v_z}]$. The inner product is defined as

$$\langle \widehat{\boldsymbol{v_1}}, \widehat{\boldsymbol{v_2}} \rangle = \frac{1}{8} \int_{-1}^{1} \widehat{\boldsymbol{v_1}}^* \widehat{\boldsymbol{v_2}} \, \mathrm{d}y. \tag{47}$$

Therefore we choose the output vector $\widehat{\boldsymbol{v}} = [\widehat{v_x} \quad \widehat{v_y} \quad \widehat{v_z}]$ and the output matrix C is defined as:

$$\begin{aligned} \widehat{\boldsymbol{v}} &= \begin{bmatrix} v_x \\ v_y \\ v_z \end{bmatrix} = \begin{bmatrix} 1 & 0 & 0 & 0 & 0 & 0 & 0 & 0 & 0 \\ 0 & 1 & 0 & 0 & 0 & 0 & 0 & 0 & 0 \\ 0 & 0 & 1 & 0 & 0 & 0 & 0 & 0 & 0 \end{bmatrix} \begin{bmatrix} M \\ 0 \end{bmatrix} \begin{bmatrix} \psi^h \\ p \end{bmatrix} && (48) \\ &\equiv C \begin{bmatrix} \psi^h \\ p \end{bmatrix} && (49) \end{aligned}$$

3.7 MATLAB implementation

Because we have used the 2D/3C model where we ignore changes in the x-direction and taken a fourier transform in z, we now have a time-evolution matrix, $\widetilde{A}$, which is operates on y alone. To solve this system of equations we can discretize all functions and write the differential and integral operators as differentiation matricies and their inverses. We utilize a MATLAB package written by Weideman and Reddy to generate differentiation matricies using spectral collocation [**?**].

4 Wall Stability Analysis

Re-write:

Before studying the coupled fluid wall system, it is useful to investigate the response of the wall by itself. In this case, we perform an input-output analysis of Eqs. 20, 21, and 22, viewing the body force f_i, $i \in \{x, y, z\}$ as the input for each equation and the wall velocities as the output vectors.

First, note that to first order in the perturbations, each component of the wall velocity is decoupled from the other two, and therefore we can study each component separately. Second, we assume that the material is translation invariant in the spanwise direction, and therefore we take a fourier transform in that direction. The resulting equation for each component can be written in the following form:

The properties of the compliant wall are determined by a rather large parameter space: the mass density of the wall σ, three damping parameters D_i, three tension parametersT_i and three *tethering* spring constants $\mathcal{J}_i$. We analyze the stability properties of the wall alone as a function of these parameters to gain intuition about how modes of the wall motion might interact with the fluid motion. First, we write the system of equations for the undriven wall positions (u_x, u_y, u_z) and velocities $(\dot{u_x} = s_x, \dot{u_y} = s_y, \dot{u_z} = s_z)$ after taking a fourier transform in the spanwise direction:

$$\partial_t \begin{bmatrix} u_x \\ u_y \\ u_z \\ s_x \\ s_y \\ s_z \end{bmatrix} = \begin{bmatrix} 0 & 0 & 0 & 1 & 0 & 0 \\ 0 & 0 & 0 & 0 & 1 & 0 \\ 0 & 0 & 0 & 0 & 0 & 1 \\ -\frac{\mathcal{J}_x + T_x k^2}{\sigma} & 0 & 0 & -D_x/\sigma & 0 & 0 \\ 0 & -\frac{\mathcal{J}_y + T_y k^2 + B_y k^4}{\sigma} & 0 & 0 & -D_y/\sigma & 0 \\ 0 & 0 & -\frac{\mathcal{J}_z + T_z k^2}{\sigma} & 0 & 0 & -D_z/\sigma \end{bmatrix} \begin{bmatrix} u_x \\ u_y \\ u_z \\ s_x \\ s_y \\ s_z \end{bmatrix} \equiv A_{wall} \begin{bmatrix} u_x \\ u_y \\ u_z \\ s_x \\ s_y \\ s_z \end{bmatrix} \tag{50}$$

This system is neutrally stable if all of the $D_i = 0$, and asymptotically stable otherwise, because it is a damped system which is not being driven. Now we can perform an input/output analysis of the system, where we imagine a body force acting upon the wall. Because we have taken a fourier transform in the spanwise direction, the transfer function $H(i\omega) = (i\omega I - A_{wall})^{-1} B$ can be determined analytically. Since body forces acting on the wall affect the time derivative of the velocities, the input matrix B is just:

$$B = \begin{bmatrix} 0 & 0 & 0 & 0 & 0 & 0 \\ 0 & 0 & 0 & 0 & 0 & 0 \\ 0 & 0 & 0 & 0 & 0 & 0 \\ 0 & 0 & 0 & 1 & 0 & 0 \\ 0 & 0 & 0 & 0 & 1 & 0 \\ 0 & 0 & 0 & 0 & 0 & 1 \end{bmatrix} \tag{51}$$

The H_∞ norm is defined as the $\sup_\omega \sqrt{\lambda_{max}(H(i\omega) * H(i\omega))}$, where $\lambda_{max}(M)$ is the maximum eigenvalue of the matrix M. It is the maximum amplification of inputs to an output over all possible inputs over all times. In this analysis we are permitting small, possibly time-varying perturbations to drive the compliant wall and looking for large resonances, which will show up as large values

of the H_∞ norm. Because the non-driven system is stable, all inputs will eventually decay as $t \to \infty$, and therefore the H_∞-norm remains finite. An analytic expression for the eigenvalues of the matrix $H(i\omega) * H(i\omega)$ is:

$$\begin{bmatrix} 0 \\ 0 \\ 0 \\ \frac{\sigma^2\left(\omega^2+1\right)}{\mathrm{Dx}^2\omega^2+(\mathrm{Tx}k^2+\sigma\omega^2-\mathrm{Jx})^2} \\ \frac{\sigma^2\left(\omega^2+1\right)}{\mathrm{Dy}^2\omega^2+(\mathrm{By}k^4-\mathrm{Ty}k^2-\sigma\omega^2+\mathrm{Jy})^2} \\ \frac{\sigma^2\left(\omega^2+1\right)}{\mathrm{Dz}^2\omega^2+(\mathrm{Tz}k^2+\sigma\omega^2-\mathrm{Jz})^2} \end{bmatrix} \tag{52}$$

We note that different components of the wall displacement do not interact with each other. Therefore the equation of motion for each component is decoupled from every other, and each non-zero eigenvalue of the $H(i\omega) * H(i\omega)$ matrix corresponds to amplification of body forces oriented parallel to either the x, y, or z planes. The larger of these three values is the $\lambda_{max}(\omega)$ in the definition for the H_∞ norm, and corresponds to the maximum amplication of any input with a specific frequency, ω. We do not wish to find $\sup_w \lambda_{max}(\omega)$ by discretizing ω and taking a maximum. This is because the resonances become increasingly sharp as the wave number k increases, and it becomes prohibitively computationally intensive. *Given that these resonances in ω are so sharp, is it possible for the fluid to drive the wall at exactly the frequency at which the wall resonates?* A better solution is to realize that these eigenvalues have simple asymptotic behavior in two separate regimes. To stress the similarity of the three eigenvalues, let $\gamma_i(k) \equiv \frac{-\mathcal{J}+k^2T_i-k^4E_i}{\sigma}$, where $E_x = E_z = 0$. Then for large k, each eigenvalue attains its maximum when $\omega^2 = \gamma(k)$. For small k, the eigenvalues attain their maxima when $\omega = 0$. The crossover between the two regimes occurs at

$$\gamma_i(k) = \frac{-1 + \sqrt{1 + 4\left(\frac{D_i}{\sigma}\right)^2}}{2} \tag{53}$$

then we can write a simple expression for the H_∞-norm which is accurate except in a small region of k-values around the crossover point, Eq. 53.

$$H_\infty(k) \simeq \max\left(\sqrt{\frac{1}{\gamma_y(k)^2}},\ \sqrt{\frac{1}{\gamma_z(k)^2}},\ \sqrt{\left(\frac{m}{Dn}\right)^2 \frac{1+\gamma_y(k)}{\gamma_y(k)}},\ \sqrt{\left(\frac{m}{Dt}\right)^2 \frac{1+\gamma_z(k)}{\gamma_z(k)}}\right) \tag{54}$$

We are now interested in the properties of this H_∞ norm as a function of the wall parameters. Presumably if the wall and the fluid are highly succeptible to perturbations of similar wavenumber in z, then they have the potential to interact in a non-trivial way, introducing feedback. *It seems that when the values for the terms in the wall-normal and tangential wall parameters are exactly the same, the system goes unstable. Why is this? There is no evidence for that behaviour in the H-infty norm of the wall alone. Perhaps something like continuity couples the two wall equations together?*

5 Notes and Remaining issues

- Note J_y must be of the same order as σ for the numerics to be well-behaved. This is because the wall velocity is only constrained by $\gamma(y)$, and this is zero if $J_y \ll \sigma$.
- Note that the equation for s_x contains a constant term, V_0. This is due to the shear stress in the fluid due to the mean flow profile. If we switch into a frame where the bottom wall is not moving, then we are switching into a frame such that $\widetilde{s_x} = \overline{s_x} - V_0$ and I think this problem goes away.*need to check*
-

6 Appendix: Harmonic potential wall model

A starting point for our 2D/3C plate-membrane model is a 2D lattice of masses connected by hookean springs in the limit that the lattice spacing goes to zero. Consider the harmonic potential energy of such a sheet oriented parallel to the x-z plane, where the lattice spacing is a, the spring constant in each direction is T_i and the index of each lattice point is n. Let the displacement field in each direction be u_i, and let all of the fields be constant in x. Then the potential energy to first order in the displacement fields is given by the following equation [1]:

$$U^{harm}(z) = \frac{1}{2} T_i \sum_n \left[u_i(na) - u_i([n+1]a)\right] \cdot \left[u_i(na) - u_i([n+1]a)\right] \tag{55}$$

Then the equation of motion for each node can be found by taking the partial derivative of the potential with respect to the displacement. For example, the equation of motion for the diplacement in z is given by

$$M\ddot{u_z}(na) + B\dot{u_z}(na) = F_z - \frac{\partial U^{harm}}{\partial u_z} = -T_z\left(-u_z([n-1]a) + 2u_z(na) - u_z([n+1]a)\right). \tag{56}$$

where M is the mass of each node, B is a damping coefficient, and F_z is external forcing. Similar equations hold for the displacements fields in the x and y directions. We now divide both sides of the equation by a^2 and take the limit that the lattice spacing goes to zero.

$$\lim_{a\to 0}\left[\sigma\ddot{u_z}(na) + D_z\dot{u_z}(na) = f_z - T_z\left(\frac{-u_z([n-1]a) + 2u_z(na) - u_z([n+1]a)}{a^2}\right)\right] \tag{57}$$

$$\sigma\ddot{u_z}(z) + D_z\dot{u_z}(z) = f_z + T_z\frac{\partial^2 u_z(z)}{\partial z} \tag{58}$$

where σ is the areal mass density of the wall, D_z is a damping coefficient density, and f_z are external stresses in the z direction. We retain the intertial term in our equation of motion because we are interested in high Reynolds number flows. Similarly, we have equations for u_y and u_x:

$$\sigma \ddot{u_x}(z) + D_x \dot{u_x}(z) = f_x + T_x \frac{\partial^2 u_x(z)}{\partial z}, \tag{59}$$

$$\sigma \ddot{u_y}(z) + D_y \dot{u_y}(z) = f_y + T_y \frac{\partial^2 u_y(z)}{\partial z}. \tag{60}$$

References

[1] Ashcroft and Mermin. *Solid State Physics.* Brooks/Cole, 1976.

[2] T. B. Benjamin. Effects of a flexible boundary on hydrodynamic stability. *J. Fluid Mech.*, 9:513, 1960.

[3] K.M. Butler and B.F. Farrell. Three-dimensional optimal perturbations in viscous shear flow. *Physics of Fluids A*, 4(8):1637–1650, 1992.

[4] P.W. Carpenter and A.D. Garrad. The hydrodynamic flow over kramer-type compliant surfaces. part 1. tollmien schlichting instabilities. *J. Fluid Mech.*, 155:465–510, 1985.

[5] R.F. Curtain and H.J. Zwart. *An introduction to Infinite-Dimensional Linear Systems Theory.* Springer-Verlag, 1995.

[6] R.W. Metcalfe. J.J. Riley, M. Gad-el-Hak. Compliant coatings. *Ann. Rev. Fluid Mech.*, 20:393–420, 1988.

[7] B. Bamieh K.M. Bobba and J.C. Doyle. Global stability and transient growth of stream-wise constant perturbations in plane couette flow. *??*, 2002.

[8] M.O. Kramer. *Readers Forum, J. Aerospace Sci.*, 27(68), 1960.

[9] M.O. Kramer. Boundary layer stabilization by distributed damping. *J. Amer.Soc. Nav. Engrs.*, 72(25), 1960.

[10] V. Kumaran. Stability of the flow of a fluid through a flexible tube at intermediate reynolds number. *J. Fluid Mech.*, 357:123–140, 1998.

[11] M.T. Landahl. On the stability of a laminar incompressible boundary layer over a flexible surface. *J. Fluid Mech.*, 13:609, 1961.

[12] V. Shankar R.M Thaokar and V. Kumaran. Effect of tangential interface motion on the viscous instability in fluid flow past flexible surfaces. *Euro. Phys. J. B*, 23:533–550, 2001.

[13] L.N. Trefethen, A.E. Trefethen, S.C. Reddy, and T.A. Driscoll. Hydrodynamic Stability Without Eigenvalues. *Science*, 261(5121):578, 1993.